



Enhancement of Cd(II) adsorption by polyacrylic acid modified magnetic mesoporous carbon



Guangming Zeng^{a,b,*}, Yuanyuan Liu^{a,b}, Lin Tang^{a,b,*}, Guide Yang^{a,b}, Ya Pang^{a,b}, Yi Zhang^{a,b}, Yaoyu Zhou^{a,b}, Zhen Li^{a,b}, Mengyan Li^c, Mingyong Lai^{a,b}, Xiaoxiao He^{a,b}, Yibin He^{a,b}

^a College of Environmental Science and Engineering, Hunan University, Changsha 410082, Hunan, PR China

^b Key Laboratory of Environmental Biology and Pollution Control (Hunan University), Ministry of Education, Changsha 410082, Hunan, PR China

^c Dept. of Civil and Environmental Engineering, Rice University, Houston, TX 77005, USA

HIGHLIGHTS

- A new adsorbent was prepared by modifying magnetic mesoporous carbon with polyacrylic acid.
- The modified materials exhibited excellent magnetic separation performance and high removal efficiency for Cd(II).
- Higher adsorption capacity was observed for the modified adsorbent than the pristine adsorbent and activated carbon.
- The modified adsorbent showed good recyclable adsorption performance.

ARTICLE INFO

Article history:

Received 30 April 2014

Received in revised form 26 July 2014

Accepted 28 July 2014

Available online 7 August 2014

Keywords:

Polyacrylic acid

Magnetic mesoporous carbon

Adsorption

Cadmium

ABSTRACT

A novel adsorbent was prepared by chelating magnetic mesoporous carbon with polyacrylic acid (PAA) to improve the performance of Cd(II) adsorption. Structure characterization demonstrated that the composites were successfully modified with carboxyl groups and preserved ordered mesostructure after modification. The high saturation magnetization (9.2 emu/g) of the modified composites indicated easy and fast separation from water under a moderate magnetic field. Batch experiments with variable pH, contact time and ionic strength were conducted to evaluate the adsorption performance. The modification accelerated the cadmium adsorption rate. The adsorption kinetics of the two materials followed pseudo-second-order model and exhibited 3-stage intraparticle diffusion mode. Equilibrium data were best described by Langmuir model, and the estimated maximum adsorption capacity for the modified adsorbent increased to 406.6 mg/g, which was 140.8% higher than the pristine materials. Moreover, the Cd(II) loaded adsorbent could be regenerated using 0.1 M ethylenediaminetetraacetic acid solution, and the regenerated adsorbent after five cycles could retain 85.2% of the adsorption capacity for the fresh adsorbent. The results suggested that PAA modified adsorbents could be considered to be very effective and promising materials for Cd(II) removal from waste water.

© 2014 Elsevier B.V. All rights reserved.

1. Introduction

Water pollution arisen during the industrialization process has become a critical environmental and economic issue worldwide [1,2]. Aqueous heavy metal pollution has particularly aroused increasing public concerns due to its widespread occurrence and potential toxicity even at low concentration [3–5]. Among heavy metals, Cadmium (Cd), as a highly toxic metal, could be released

into the environment through industrial waste mainly from metallurgical alloying, lead–zinc mining, electroplating, photography, pigment works, and production of alkaline batteries [6]. Exposure to elevated level of Cd could cause acute and chronic disorders on the nervous system, kidney, liver and cardiovascular system [7], therefore, efficient removal of Cd is of particular concern.

A wide variety of techniques, including precipitation, filtration, ion exchange, reverse osmosis, membrane separation, solvent extraction and adsorption, have been developed to remove aqueous heavy metals [7]. Among these techniques, adsorption is generally considered as one of the most promising and frequently used techniques due to its easy operation, high efficiency and economical advantages [8,9]. In particular, for the treatment of a large

* Corresponding authors at: College of Environmental Science and Engineering, Hunan University, Changsha 410082, Hunan, PR China. Tel.: +86 731 88822754; fax: +86 731 88823701.

E-mail addresses: zgming@hnu.edu.cn (G. Zeng), tanglin@hnu.edu.cn (L. Tang).

amount of waste water with low concentration of Cd(II), adsorption is considered as most cost-effective.

The key to the adsorption techniques lies in the efficiency and effectiveness of the adsorbent, which requires the adsorbent with high surface area for more binding sites and strong affinity to sorbate. Among the numerous adsorbents used for heavy metal removal, activated carbon-based adsorbents have been most widely used because of their large surface area, good adsorption performance and economic advantages [10,11]; however, with a large fraction of micropores (<2 nm) occupying most pore volume in the activated carbons, their application in adsorption can be limited by slow diffusion kinetics, relatively low adsorption capacity and hydrothermal stability [12]. Compared with traditional adsorbents such as activated carbon, mesoporous materials, with their particular properties such as large surface areas, high pore volumes, regular mesopores and higher hydrothermal stability [12,13], have been proved to be very promising adsorbents for the removal of a large variety of pollutants [10].

Easy operation is also a very essential property for the ideal adsorbent. Magnetic separation technology, in comparison with other methods such as centrifugation, precipitation and filtration, has exhibited easy operation and reduced capital costs [14,15]. Therefore, the hybrid systems with magnetic nanoparticles and the porous materials have been extensively used in the adsorption process to improve separation after water treatment.

Recently, modifying the inorganic adsorbent with functional organic groups has been necessary to afford more binding areas and improve adsorption performance [16–18]. Unlike the instable low-molecular-weight amino-, carboxyl- or thiol-containing species, polymers with heavier functional group such as polyethylenimine (PEI) [19] or polyacrylic acid (PAA) [20], are more stable and can deliver high binding capacity because of its high density of carboxyl-containing or imine-containing species. Although there have been extensive industrial and academic interests in the studies of the polymer/inorganic nanoparticles recently [19,20], few of them have focused on the polymer/mesoporous carbon composites. Moreover, to the best of our knowledge, there has been no report focused on the preparation and application of PAA loaded magnetic mesoporous carbon.

In the present work, we have synthesized PAA chelated magnetic mesoporous carbon (PAA-MMC) and compared its adsorption properties with magnetic mesoporous carbon (MMC). Sorption kinetics and isotherms of the two adsorbents were investigated, and effects of pH and ionic strength on adsorption properties were also evaluated. To compare the adsorption capacity of PAA-MMC with traditional porous adsorbent, the adsorption capacities of Pb(II), Zn(II), Cu(II) and Cd(II) by PAA-MMC, MMC and activated carbon were also studied.

2. Materials and methods

2.1. Materials

Pluronic copolymer P123 (EO₂₀PO₇₀EO₂₀) (M_{av} = 5800) and polyacrylic acid (35%, M_{av} = 1 × 10⁵) were purchased from Sigma-Aldrich (USA). All other chemicals were of analytical grade and were used as received without further purification.

2.2. Synthesis of adsorbents

Magnetic mesoporous carbon (MMC) was prepared according to a co-impregnation method [21]. Typically, the mesostructured SBA-15 silica template was first prepared as described previously [22]. And then a multi-component solution containing 0.8 mmol Fe(NO₃)₃·9H₂O, 0.8 mmol Ni(NO₃)₂·6H₂O, 0.5 mL ethanol and

1 mL furfuryl alcohol was prepared. After infiltrating 1.4 mL of the solution into 1.2 g SBA-15 template, the impregnated mixture was cured at 80 °C in air for 10 h, followed by carbonization and reduction of the metal oxides under a 5% H₂–95% Ar atmosphere at 900 °C for 2 h. The resulted product was washed by heated 2 M NaOH solution and water and dried at 70 °C to get MMC. PAA-MMC was synthesized under optimized conditions based on the method mentioned before [23]. Typically, 0.5 g of MMC was mixed with 1 L of solution containing 1.5 g PAA under pH 5.0 and agitated for 24 h. The mixture was then filtered, washed and then stored for the future use.

2.3. Characterization

N₂ adsorption-desorption isotherms were obtained on a Micromeritics 2020 analyzer at 77 K. The surface area was determined based on BET analyses. Pore size distribution were derived from the desorption branches of the isotherms based on BJH model, and the total pore volume was calculated using BJH analyses. Transmission electron microscopy (TEM) images were performed on a JEOL-1230 electron microscope operated at 100 kV. FTIR spectrometer (WQF-410) was applied to characterize the carboxyl groups chelated on MMC. Zeta Potential was measured by first dispersing MMC and PAA-MMC in 1 mmol/L NaCl solution by sonication, and then determining the supernatant with Zetasizer Nano (ZEN3600, Malvern). The magnetic properties of the samples were studied by a vibrating sample magnetometer (VSM) at 25 °C.

2.4. Batch adsorption test

The batch mode adsorption studies were carried out by agitating 5 mg of MMC or PAA-MMC in 25 mL of Cd(II) solution prepared with Cd(NO₃)₂ on a shaker at 150 rpm under controlled temperature of 30 °C. The solution pH was adjusted using HCl or NaOH solutions. At each predetermined time point, the adsorbent was separated from the upper solution with magnetism, and then the residual concentration of Cd(II) was measured by atomic absorption spectroscopy (AAS Hitachi Z-8100, Japan).

The adsorption capacity of Cd(II) in the adsorption system, q_e , was calculated by

$$q_e = \frac{(C_i - C_e)V}{m} \quad (1)$$

where C_i and C_e are initial and equilibrium concentrations (mg/L), respectively; m is the mass of the adsorbent (g); and V is volume of the solution (L). Experiments were carried out in duplicate, and the arithmetic mean values were calculated, with the standard deviations less than 5%.

Effects of pH and ionic strength on the adsorption process were studied with Cd(II) concentration of 100 mg/L and equilibrium time of 2 h. Sodium chloride and calcium nitrate solutions from 50 to 500 mg/L were maintained in the adsorption system to study the effect of ionic strength on Cd(II) sorption. To compare the metal removal capabilities of PAA-MMC, MMC and activated carbon, adsorption system containing 800 mg/L of Pb(II), Zn(II), Cu(II) and Cd(II) were used.

2.5. Adsorption kinetics

Sorption kinetics were investigated to evaluate both the rate of Cd(II) sorption and the equilibrium time required for the sorption isotherm. The experiments were conducted under initial Cd(II) concentration of 100 mg/L. Adsorption rate were analyzed using two kinetic models, i.e., the pseudo-second-order model and the intraparticle diffusion model.

The pseudo-second-order kinetic model is expressed by the equation

$$\frac{t}{q_t} = \frac{1}{k_{ad}q_e^2} + \frac{1}{q_e}t \quad (2)$$

where q_e and q_t are the amount of metals adsorbed at the equilibrium and time t , respectively (mg/g), and k_{ad} is the pseudo-second-order rate constant for the adsorption process (mg/g min).

The intraparticle diffusion model is described by the equation

$$q_t = k_{id}t^{0.5} \quad (3)$$

where q_t stands for the amount of heavy metals adsorbed (mg/g) at time t , and k_{id} is the intraparticle diffusion rate constant (mg/g h^{1/2}).

2.6. Adsorption isotherms

Sorption isotherms were measured for MMC and PAA-MMC by varying Cd(II) concentration from 50 to 1200 mg/L. After 2 h of equilibrium, the suspension was sampled and separated with magnetism, and the filtrate was analyzed for Cd(II).

Langmuir and Freundlich isotherm models were used to evaluate the adsorption isotherm. The Langmuir equation can be defined as

$$\frac{C_e}{q_e} = \frac{1}{bq_m} + \frac{C_e}{q_m} \quad (4)$$

where q_e is the equilibrium adsorption capacity (mg/g), C_e is the concentration of heavy metals at equilibrium (mg/L), q_m is the maximum adsorption capacity (mg/g), and b stands for the equilibrium adsorption constant (L/mg).

Based on the further analysis of Langmuir model, the adsorption system can be evaluated by the dimensionless parameter (R_L), which is defined as

$$R_L = \frac{1}{1 + bC_0} \quad (5)$$

where C_0 is the initial concentration of the heavy metal. According to the value of R_L , the adsorption process can be evaluated as irreversible ($R_L = 0$), favorable ($0 < R_L < 1$), linear ($R_L = 1$) and unfavorable ($R_L > 1$).

The Freundlich isotherm model is expressed as

$$q_e = K_F C_e^{1/n} \quad (6)$$

where C_e stands for the Freundlich constant indicating adsorption capacity, and n is the heterogeneity factor related to the adsorption intensity of the adsorbent.

2.7. Desorption and regeneration of adsorbent

The feasibility of desorption and regeneration of the adsorbent was investigated using 0.1 M EDTA. After agitating 5 mg of PAA-MMC with 25 ml of Cd(II) solution (initial concentration of 100 mg/L) under optimum conditions, Cd(II) loaded adsorbent was washed, dried and added into 25 ml of 0.1 M ethylenediaminetetraacetic acid (EDTA) solution for desorption at 150 rpm at 30 °C for 24 h. The adsorbent was magnetically separated, washed and dried for the successive adsorption–desorption cycles.

3. Results and discussion

3.1. Characterization

From the TEM image of Fig. 1a, large domains of ordered stripe-like structures were observed for MMC, and magnetic nanoparticles were found embedded in the carbon rods over the entire

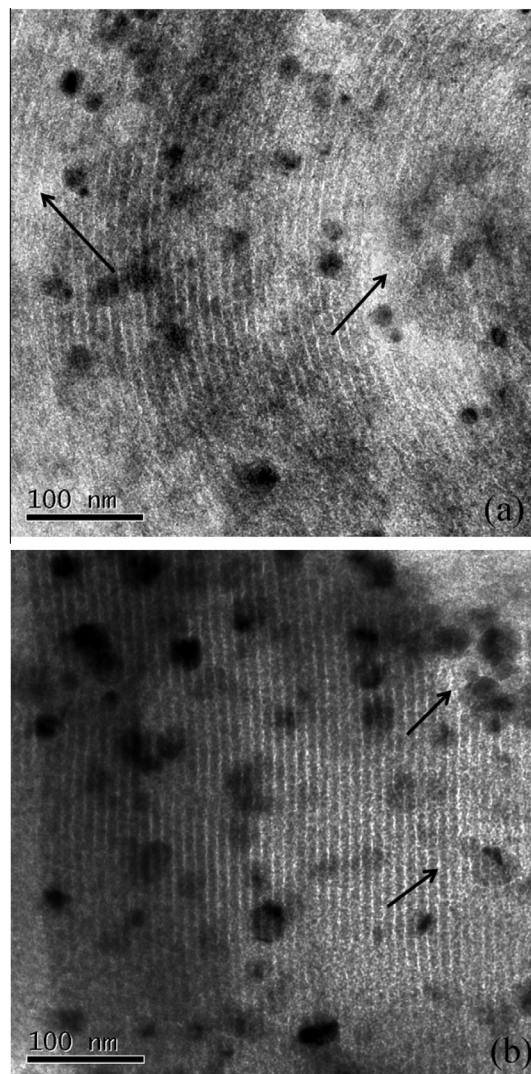


Fig. 1. TEM images of (a) MMC and (b) PAA-MMC.

MMC particles. Large voids resulted from some broken nanorods (indicated with arrows) could also be observed, corresponding to the secondary mesopores of the composite [24], which could be further convinced by BET and BJH analyses. As demonstrated in Fig. 1b, PAA-MMC has retained the 2-D hexagonal mesostructure of MMC, and nanoparticles and voids were also found in PAA-MMC, indicating the PAA chelating did not destroy the structure of MMC.

Two obvious hysteresis loops could be observed in the isotherm curve (Fig. 2a), indicating the existence of two pore systems in both MMC and PAA-MMC [25]; and the corresponding pore size distributions (Fig. 2b), showing two pore systems centered at 4.0 nm and 18.0 nm, the other at 3.0 nm and 5.0 nm for MMC and PAA-MMC, respectively, also confirmed the existence of bimodal systems. According to Table 1 and Fig. 2b, the pore volume and the centered pore sizes decreased with the loading of PAA, indicating that PAA was successfully modified inside the pores of MMC. FTIR spectroscopic analysis (Fig. 3) of both MMC and PAA-MMC further confirmed the structure of the composites. For both of the materials, the characteristic peaks at 1120 cm⁻¹, 1640 cm⁻¹ and 3448 cm⁻¹, representing C–O, –OH and H–O–H stretch vibrations, respectively, were observed. A group of peaks around 2350 cm⁻¹ for both MMC and PAA-MMC might be due to carbon dioxide or C≡C in-line deformation vibrations [4]. New signal at 1720 cm⁻¹ representing carboxyl group was clearly observed in

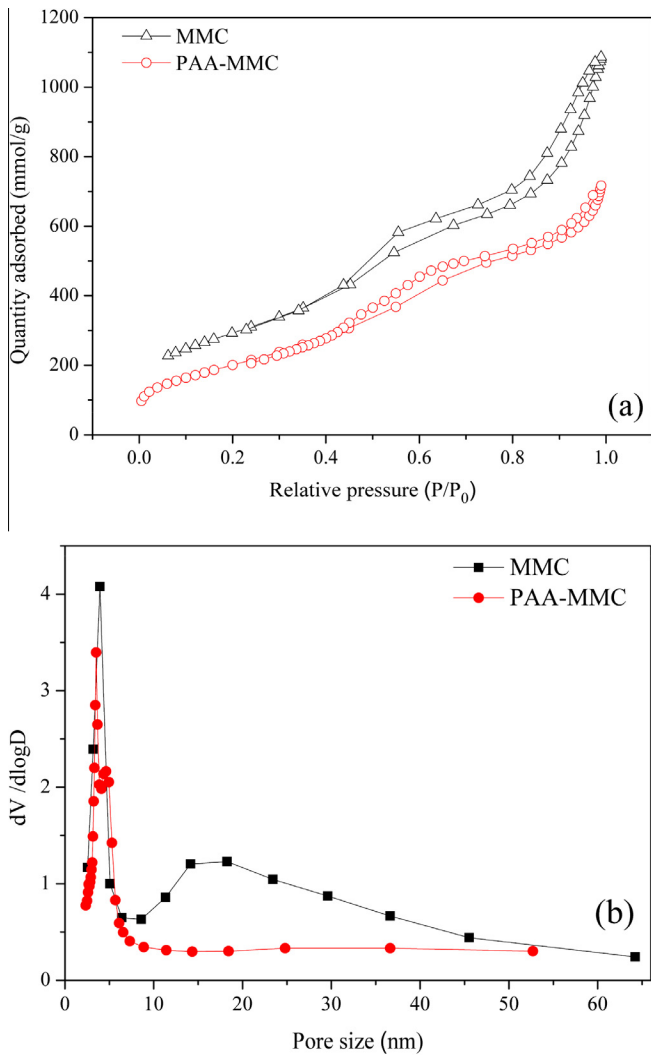


Fig. 2. (a) Nitrogen adsorption–desorption isotherms and (b) the corresponding pore size distributions of PAA-MMC and MMC.

Table 1
Pore structure parameters of MMC and PAA-MMC.

Sample	S_{BET} (m ² /g)	S_{BJH} (m ² /g)	V_{BJH} (cm ³ /g)	Pore size (nm)
MMC	1058.7	1092.2	1.79	5.0, 18.0
PAA-MMC	689.7	779.6	0.99	3.0, 5.0

PAA-MMC, which confirms that MMC were successfully chelated with PAA [26], and the difference of zeta potentials (Fig. 4) between MMC and PAA-MMC also supported this observation. The isoelectric point of MMC was pH = 3.18, while the isoelectric point of PAA-MMC shifted to pH = 4.74. In a neutral solution, both of the composites were negatively charged, which could adsorb positively charged ions such as Cd²⁺.

Fig. 5 shows the magnetization curves of MMC and PAA-MMC. The corresponding magnetization saturation values for MMC and PAA-MMC were 11.8 and 9.2 emu/g, respectively. Although magnetization strength decreased after PAA chelating, it could be inferred that the separation of PAA-MMC in aqua media could be controlled by magnetic fields with its magnetization strength [25]. And according to the inset of Fig. 5, PAA-MMC after adsorption could be effectively separated from the liquid phase using an outer magnet, further demonstrating the magnetic properties of PAA-MMC.

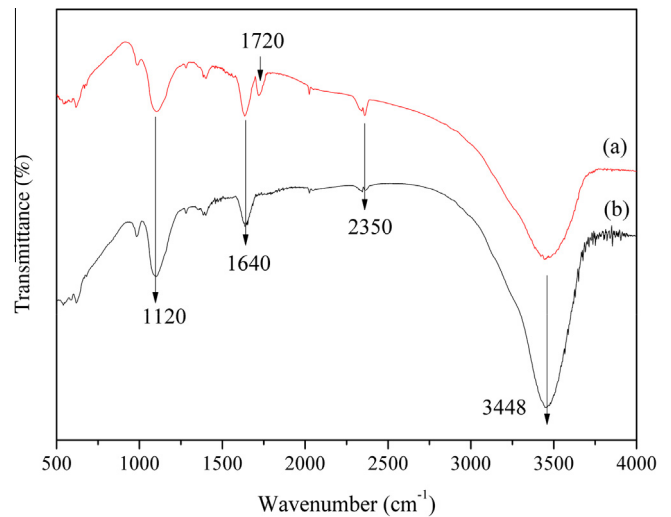


Fig. 3. Fourier transform-infrared (FT-IR) spectra of (a) PAA-MMC and (b) MMC.

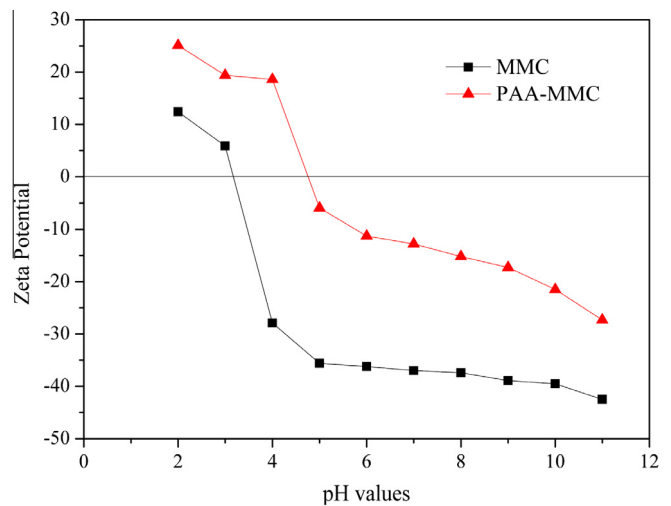


Fig. 4. Zeta potentials of PAA-MMC and MMC as a function of solution pH.

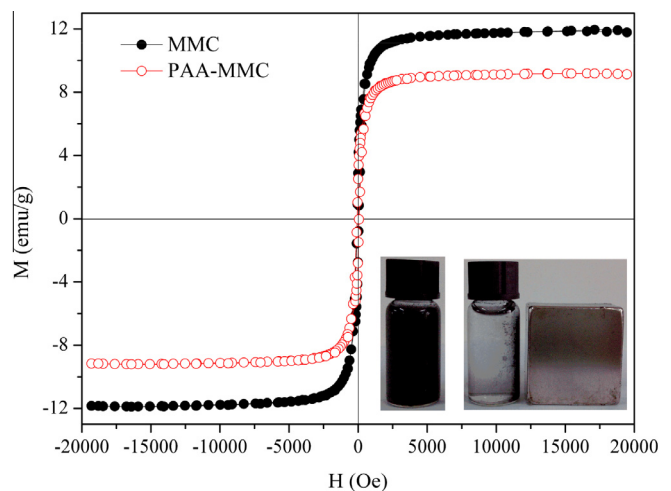


Fig. 5. Magnetization curves of PAA-MMC and MMC. Inset is a photograph of PAA-MMC after Cd(II) adsorption in aqueous solution before (left) and after (right) being attracted by an outer magnet (adsorbent dosage 20 mg/L, initial concentrations of metal ions 100 mg/L, pH 7.0, contact time 2 h, temperature 30 °C).

3.2. Adsorption kinetics

Fig. 6a shows the time dependent data of Cd(II) adsorption by MMC and PAA-MMC. As shown in Fig. 6a, the equilibrium for both of the two adsorbents was achieved within 2 h. The pseudo-second-order kinetic model (inset of Fig. 6a) was used to investigate the adsorption kinetics, with the constant k_{ad} calculated and listed in Table 2. The pseudo-second-order model showed good

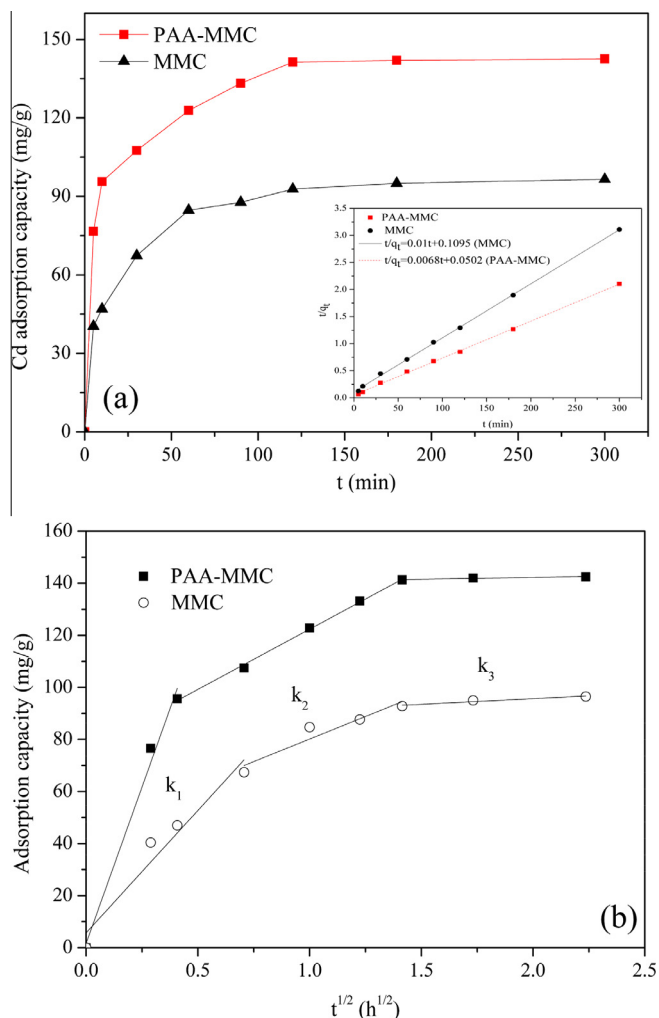


Fig. 6. (a) Adsorption kinetics of Cd(II) by PAA-MMC and MMC, the inset picture is the pseudo-second-order adsorption plot. (b) The intra-particle diffusion rate constants of Cd(II) adsorption by PAA-MMC and MMC (adsorbent dosage 20 mg/L, initial concentrations of metal ions 100 mg/L, pH 7.0, temperature 30 °C).

Table 2
Pseudo-second-order and intraparticle diffusion parameters.

Adsorbents	$q_{e,cal}^a$ (mg/g)	$q_{e,exp}^b$ (mg/g)	k_{ad} (mg/g min)	R^2		
<i>Pseudo-second-order parameters</i>						
MMC	96.5	96.5	0.91	0.9995		
PAA-MMC	143.5	142.5	1.02	0.9991		
Adsorbents	$k_{id,1}$ (mg/g h ^{1/2})	R^2	$k_{id,2}$ (mg/g h ^{1/2})	R^2	$k_{id,3}$ (mg/g h ^{1/2})	R^2
<i>Intraparticle diffusion parameters</i>						
MMC	94.0	0.9242	34.7	0.8747	4.4	0.8881
PAA-MMC	240.0	0.9800	46.3	0.9975	1.4	0.8996

^a The calculated adsorption capacity at equilibrium, namely q_e in Eq. (5).

^b The measured adsorption capacity at equilibrium.

fitting to the Cd(II) adsorption data with excellent correlation coefficients ($R^2 > 0.999$), and good agreement between experimental ($q_{e,cal}$) and calculated ($q_{e,exp}$) values were also exhibited in Table 2. Thus it could be indicated that both of the adsorption rates of the two composites were controlled by chemical process [11]. The rate constant (k_{ad}) of PAA-MMC was relatively higher than that of MMC, and a significant difference in Cd(II) adsorption rates ($p < 0.01$) between the pristine and PAA-modified MMC was confirmed with statistical analysis, indicating that faster uptake of Cd(II) onto the adsorbent could be obtained by the grafting of PAA. Faster adsorption rate might be caused by the smaller diffusion path as PAA might block the pores of MMC and the diffusion of metal ions into inner surface and pores would be shortened [27].

To further evaluate the mechanism and rate-controlling steps affecting the adsorption kinetics, intraparticle diffusion model has been applied to investigate the adsorption process [18]. As shown in Fig. 6b, the plots of q_t versus $t_{1/2}$ for adsorption of Cd(II) by MMC and PAA-MMC were found to be multi-linear. The intraparticle diffusion constants were calculated and listed in Table 2. According to Table 2, it could be observed that the order of adsorption rate was $k_{id,1} > k_{id,2} > k_{id,3}$. At the beginning, Cd(II) was adsorbed by the exterior surface of both MMC and PAA-MMC, and the first stage was the instantaneous diffusion period (slope $k_{id,1}$), during which nearly 70% of Cd(II) were adsorbed by both of the composites. When adsorption on exterior surface reached saturation, the heavy metal ions entered into the mesopores of MMC and PAA-MMC. With Cd(II) diffusing in the pores of the composites, the diffusion resistance increased, resulting in the decrease of diffusion rates ($k_{id,2}$). The final stage was the equilibrium period, during which the intraparticle diffusion rate ($k_{id,3}$) slowed down and reached equilibrium [28].

3.3. Adsorption isotherms

The adsorption isotherms of Cd(II) by MMC and PAA-MMC with corresponding Langmuir plots are presented in Fig. 7. Freundlich isotherm was also used to normalize the adsorption data, and the results using both Langmuir and Freundlich isotherms were summarized in Table 3. As reflected with correlation coefficients in Table 3, both Langmuir and Freundlich model fitted well with the adsorption data ($R^2 > 0.90$), but the isotherm data for both of the adsorbents were better described by the Langmuir model compared to the Freundlich model. Since monolayer adsorption on adsorbents is assumed in Langmuir model, better fitting with this model might suggest that the existence of homogeneous active sites within both of the adsorbents and the monolayer adsorption of Cd(II) on both of MMC and PAA-MMC [29]. Moreover, the dimensionless constant R_L ranged from 0.1 to 0.728 for PAA-MMC and from 0.106 to 0.741 for MMC, so the adsorption by both of the adsorbents could be considered as favorable [30].

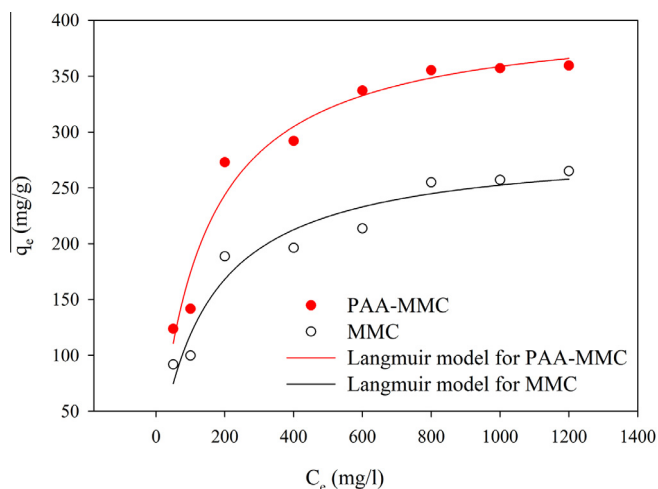


Fig. 7. Comparison of the experimental data and the model results using Langmuir isotherms for the adsorption of Cd(II) by PAA-MMC and MMC (adsorbent dosage 20 mg/L, contact time 2 h, pH 7.0, temperature 30 °C).

Table 3
Isotherm parameters for the adsorption of Cd(II) by PAA-MMC and MMC.

	Langmuir model			Freundlich model		
	q_m (mg/g)	b (L/mg)	R^2	K_F	n	R^2
MMC	288.7	0.0070	0.942	28.4	3.12	0.935
PAA-MMC	406.6	0.0075	0.964	44.8	3.28	0.903

As shown in Table 3, the estimated maximum cadmium adsorption capacity q_m of PAA-MMC was 406.6 mg/g, which was much higher than that of MMC (288.7 mg/g), though the specific surface area of PAA-MMC was reduced after the modification of polymer. Such uncorrelated relationship between specific surface area and adsorption capacity was in agreement with other studies [30]. The higher adsorption capacity of PAA-MMC might be resulted from increased binding area after the successful surface functionalization of MMC with a large number of carboxyl groups, and higher adsorption capacity after chemical modification has also been reported in other studies [31,32].

3.4. Effect of pH

The pH value of solution has been recognized as a very important parameter affecting metal adsorption process. The removal of Cd(II) as a function of pH was studied by varying the pH of solution over range of 2.0–9.0. As shown in Fig. 8, the amounts of Cd(II) adsorbed onto MMC and PAA-MMC both experienced a rapid rise at pH 2.0–4.0, followed by a slow increase over the pH range of 4.0–9.0. The maximum adsorption capacity of the two composites was both noted at pH 9.0. However, Cd(II) started to precipitate out from the solution when the pH value was over 7, thus pH 7.0 was the optimum pH value for Cd(II) adsorption.

The effect of pH on Cd(II) adsorption can be explained by point of zero charge (PZC) of the adsorbents, at which the adsorbent is neutral. When the solution pH is below PZC, the surface charge of the adsorbent is positive, restricting the approach of Cd(II) as a result of repulsive force. Since PZC of MMC and PAA-MMC was found to be around 3 and 4, respectively, both of the adsorbents were positively charged; and H^+ ions would strongly compete with Cd^{2+} for the active sites on the adsorbent when pH was under 4, resulting in the lower uptake of Cd(II) at pH under 4. When pH was above 4, both MMC and PAA-MMC were negatively charged,

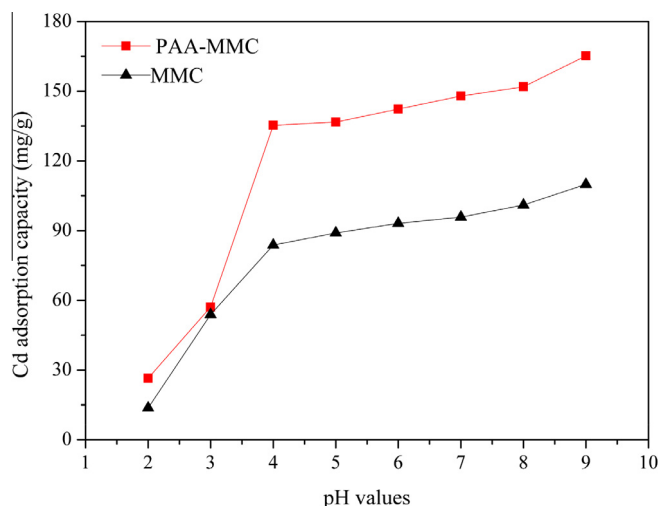


Fig. 8. Effect of pH on adsorption of Cd(II) by PAA-MMC and MMC (adsorbent dosage 20 mg/L, initial concentrations of metal ions 100 mg/L, contact time 2 h, temperature 30 °C).

and Cd(II) ions were positively charged, hence adsorption could be driven by electrostatic interaction between Cd(II) and the adsorbent [6]. Moreover, the competition of H^+ ions for active sites were decreased with the increase of pH, explaining why the adsorption capacity was increased when pH value went up from 4 to 7. However, when pH was above 7, the competition of H^+ ions could be neglected, and the augmentation of adsorption capacity was due to the precipitation of Cd(II). The observance of effects of pH on Cd(II) adsorption in this study was in accordance with previous findings [30].

3.5. Effect of ionic strength

It is common that wastewater contains significant amount of cations and anions. The presence of these ions often indicates potential competition for active adsorption sites of the adsorbents, and thus might prohibit the adsorption of Cd(II). The influence of commonly coexisting ions on the removal of Cd(II) was studied at varying concentrations of NaCl and $Ca(NO_3)_2$. Fig. 9 suggested the negative effect of the external electrolytes on the adsorption of Cd(II) on PAA-MMC. It could be indicated that increasing the concentration of common ions slightly reduced the equilibrium adsorption capacity. At an initial Cd(II) concentration of 100 mg/L, nearly 80% of the equilibrium adsorption capacity could be maintained when NaCl or $Ca(NO_3)_2$ was as high as 500 mg/L in the adsorption system. As the increasing external electrolyte would impose negative effects on adsorption capacity if the driving force of adsorption was electrostatic interaction, it could be inferred that the electrostatic interaction between PAA-MMC and Cd(II) played an important role in adsorption [33,34]. As ions that form outer-sphere surface complexes showed decreasing adsorption capacity with increasing ionic strength [35], our results also indicated the formation of outer-sphere surface complexes by the ions that adsorbed on PAA-MMC.

3.6. Comparison with other heavy metal adsorbents

To compare the adsorption performance with other adsorbents for the other heavy metals, 800 mg/L of Pb^{2+} , Zn^{2+} , Cu^{2+} and Cd^{2+} ions from homoionic solutions were used to study the equilibrium adsorption capacity (q_e) of PAA-MMC, MMC and activated carbon (AC), and the results were shown in Fig. 10. It was observed that the q_e value (mg/g) ranged from 253.2 to 317.4 for MMC, and

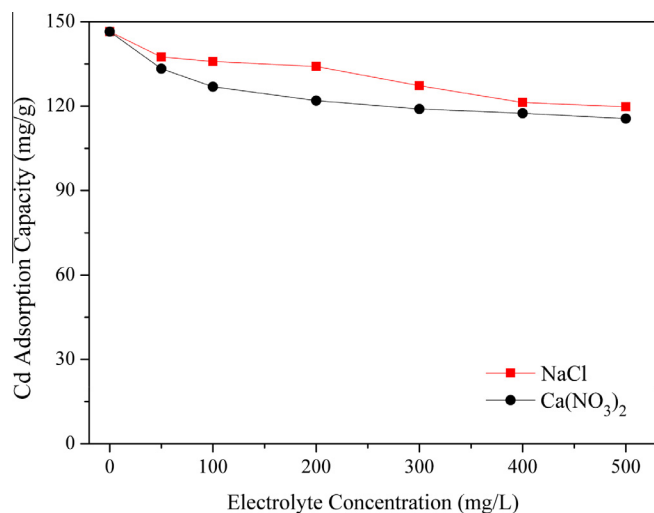


Fig. 9. Effect of common salts on the Cd(II) adsorption capacity by PAA-MMC (adsorbent dosage 20 mg/L, initial concentrations of metal ions 100 mg/L, contact time 2 h, pH 7.0, temperature 30 °C).

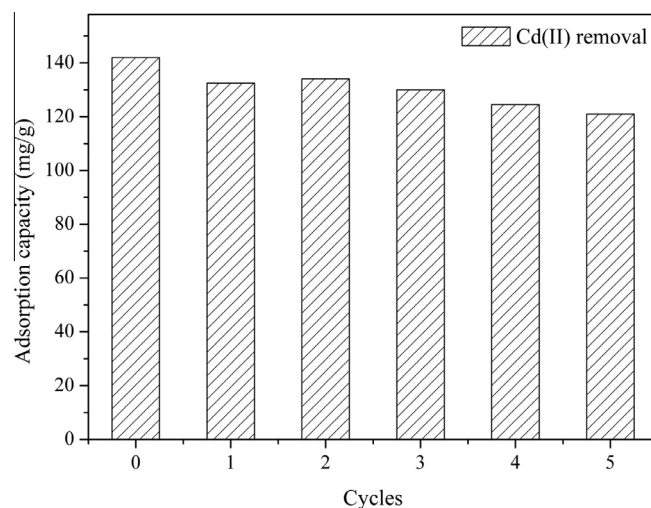


Fig. 11. Adsorption capacity of regenerated PAA-MMC for five consecutive adsorption-desorption cycles.

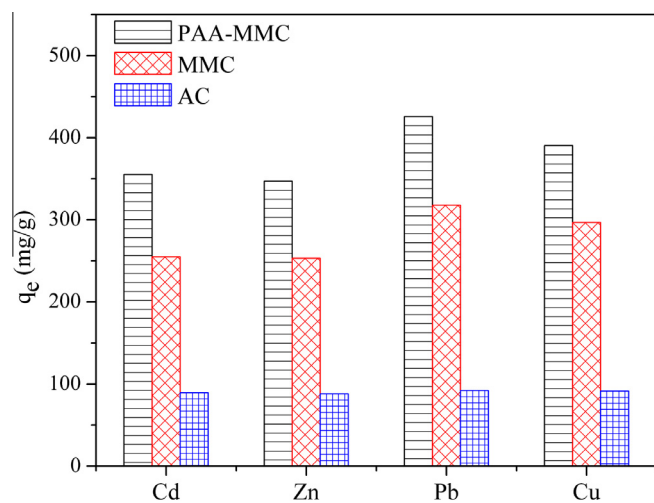


Fig. 10. Equilibrium adsorption capacities of Pb(II), Zn(II), Cu(II) and Cd(II) by PAA-MMC, MMC and AC (adsorbent dosage 20 mg/L, initial concentrations of metal ions 800 mg/L, contact time 2 h, pH 7.0, temperature 30 °C).

from 347.1 to 425.6 for PAA-MMC. The adsorption performance for all the heavy metals were greatly enhanced with respect to MMC modified by PAA, which might be due to the combination of mesoporous structure and more active adsorption sites after PAA

modification. Higher adsorption capacity was also observed in mesoporous carbon materials than in AC, with the q_e value for all the heavy metals by MMC and PAA-MMC nearly 3 and 4 times higher than that by AC, respectively, indicating that mesoporous carbons were more effective in heavy metal adsorption than AC.

For further comparison with other adsorbents, adsorption capacity of Cd(II) by several different adsorbents reported in the literature was listed in Table 4. Compared with the other alternative adsorbents, it was obvious that PAA-MMC exhibited higher adsorption capacity than most of the materials reported in the literature, indicating that PAA-MMC was a more promising candidate for effective adsorption of Cd(II) in aqueous solutions.

3.7. Regeneration of PAA-MMC

In addition to the excellent adsorption performance, regeneration and reuse of adsorbents is essential for the economic use. In this study, regeneration experiments for PAA-MMC were carried out using 0.1 M EDTA, and the successive adsorption-desorption cycles are shown in Fig. 11. The adsorption capacity decreased gradually with the increase of the cycles. However, the loaded amount of Cd(II) by regenerated PAA-MMC after five cycles was 85.2% of the amount by the fresh adsorbent, demonstrating that PAA-MMC could be regenerated and reused using EDTA.

4. Conclusions

In this study, a functional polymer-carbon composite PAA-MMC was prepared and used as an effective adsorbent to improve Cd(II)

Table 4

Comparison of maximum adsorption capacity (q_m) for adsorption of Cd(II) by various adsorbents reported in the literature.

Adsorbent	pH	q_m (mg/g)	Refs.
Functionalized graphene	6.2	73.42	[27]
Multiwalled carbon	5.0	10.86	[36]
Activated alumina	5.0	35.06	[37]
Activated carbon from coconut coirpith	5.0	93.2	[38]
Mungbean husk	5.0	34.85	[39]
NH ₂ -MCM-41	5	79.8	[40]
Fungal biomass with grafted polyacrylic acid	5	210.19	[20]
Cetylpyridinium chloride modified mesoporous carbon	8	187.7	[3]
Titanate nanotubes	5.0–6.0	238.61	[30]
Nano-hydroxyapatite	5.5	64.1	[9]
MMC	7.0	288.7	This study
PAA-MMC	7.0	406.6	This study

adsorption process. The physicochemical analysis data indicated that the composites were successfully functionalized with carboxyl groups and maintained ordered mesoporous structure and superparamagnetic behavior. The adsorption rate was accelerated after modification, and the adsorption kinetics of pristine and functionalized composites were well described by pseudo-second-order kinetic and intraparticle diffusion model. Langmuir model was most appropriate to fit the adsorption data, and the functionalized composite exhibited higher maximum monolayer adsorption capacity than the pristine material. Both of MMC and PAA-MMC exhibited better performance in neutral pH conditions, and the adsorption behavior was slightly impacted by increasing ionic strength. Compared with a lot of adsorbents reported, PAA-MMC exhibited higher adsorption capacity. Moreover, PAA-MMC could be regenerated and reused using EDTA. In conclusion, polymer modification improved adsorption behaviors and PAA-MMC could be considered as a promising adsorbent for aqueous heavy metal removal.

Acknowledgements

The study was financially supported by Program for the Outstanding Young Talents of China, the National Natural Science Foundation of China (51378190, 51039001 and 51222805), the Program for New Century Excellent Talents in University from the Ministry of Education of China (NCET-11-0129), Interdisciplinary Research Project of Hunan University, the Fundamental Research Funds for the Central Universities, Hunan University and the Program for Changjiang Scholars and Innovative Research Team in University (IRT-13R17).

References

- [1] G. Zeng, M. Chen, Z. Zeng, Risks of neonicotinoid pesticides, *Science* 6139 (2013) 1403.
- [2] G. Hu, J. Li, G. Zeng, Recent development in the treatment of oily sludge from petroleum industry: a review, *J. Hazard. Mater.* 261 (2013) 470–490.
- [3] A. Yazdankhah, S. Moradi, S. Amirmahmoodi, M. Abbasian, S.E. Shoja, Enhanced sorption of cadmium ion on highly ordered nanoporous carbon by using different surfactant modification, *Microporous Mesoporous Mater.* 1 (2010) 45–53.
- [4] L. Tang, G.D. Yang, G.M. Zeng, Y. Cai, S.S. Li, Y.Y. Zhou, Y. Pang, Y.Y. Liu, Y. Zhang, B. Luna, Synergistic effect of iron doped ordered mesoporous carbon on adsorption-coupled reduction of hexavalent chromium and the relative mechanism study, *Chem. Eng. J.* 239 (2014) 114–122.
- [5] G. Zeng, M. Chen, Z. Zeng, Shale gas: surface water also at risk, *Nature* 7457 (2013) 154.
- [6] S.M. Lee, C. Laldawngliana, D. Tiwari, Iron oxide nano-particles-immobilized-sand material in the treatment of Cu(II), Cd(II) and Pb(II) contaminated waste waters, *Chem. Eng. J.* 195 (2012) 103–111.
- [7] W.W. Tang, G.M. Zeng, J.L. Gong, J. Liang, P. Xu, C. Zhang, B.B. Huang, Impact of humic/fulvic acid on the removal of heavy metals from aqueous solutions using nanomaterials: a review, *Sci. Total Environ.* 468 (2014) 1014–1027.
- [8] J.L. Gong, B. Wang, G.M. Zeng, C.P. Yang, C.G. Niu, Q.Y. Niu, W.J. Zhou, Y. Liang, Removal of cationic dyes from aqueous solution using magnetic multi-wall carbon nanotube nanocomposite as adsorbent, *J. Hazard. Mater.* 2 (2009) 1517–1522.
- [9] Z. Zhang, M. Li, W. Chen, S. Zhu, N. Liu, L. Zhu, Immobilization of lead and cadmium from aqueous solution and contaminated sediment using nano-hydroxyapatite, *Environ. Pollut.* 158 (2010) 514–519.
- [10] A. Shahbazi, H. Younesi, A. Badiei, Functionalized SBA-15 mesoporous silica by melamine-based dendrimer amines for adsorptive characteristics of Pb(II), Cu(II) and Cd(II) heavy metal ions in batch and fixed bed column, *Chem. Eng. J.* 2 (2011) 505–518.
- [11] Y. Pang, G. Zeng, L. Tang, Y. Zhang, Y. Liu, X. Lei, Z. Li, J. Zhang, Z. Liu, Y. Xiong, Preparation and application of stability enhanced magnetic nanoparticles for rapid removal of Cr(VI), *Chem. Eng. J.* 175 (2011) 222–227.
- [12] C. Liang, Z. Li, S. Dai, Mesoporous carbon materials: synthesis and modification, *Angew. Chem. Int. Ed.* 47 (2008) 3696–3717.
- [13] L. Tang, Y. Zhou, G. Zeng, Z. Li, Y. Liu, Y. Zhang, G. Chen, G. Yang, X. Lei, M. Wu, A tyrosinase biosensor based on ordered mesoporous carbon–Au/|l-lysine/Au nanoparticles for simultaneous determination of hydroquinone and catechol, *Analyst* 12 (2013) 3552–3560.
- [14] Y. Zhang, G.M. Zeng, L. Tang, D.L. Huang, X.Y. Jiang, Y.N. Chen, A hydroquinone biosensor using modified core–shell magnetic nanoparticles supported on carbon paste electrode, *Biosens. Bioelectron.* 22 (2007) 2121–2126.
- [15] P. Xu, G.M. Zeng, D.L. Huang, C.L. Feng, S. Hu, M.H. Zhao, C. Lai, Z. Wei, C. Huang, G.X. Xie, Use of iron oxide nanomaterials in wastewater treatment: a review, *Sci. Total Environ.* 424 (2012) 1–10.
- [16] A.M. Donia, A.A. Atia, W.A. Al-amrani, A.M. El-Nahas, Effect of structural properties of acid dyes on their adsorption behaviour from aqueous solutions by amine modified silica, *J. Hazard. Mater.* 2 (2009) 1544–1550.
- [17] S. Shen, P.S. Chow, S. Kim, K. Zhu, R.B. Tan, Synthesis of carboxyl-modified rod-like SBA-15 by rapid co-condensation, *J. Colloid Interface Sci.* 2 (2008) 365–372.
- [18] G. Li, Z. Zhao, J. Liu, G. Jiang, Effective heavy metal removal from aqueous systems by thiol functionalized magnetic mesoporous silica, *J. Hazard. Mater.* 1 (2011) 277–283.
- [19] A. Heydari-Gorji, Y. Belmabkhout, A. Sayari, Polyethylenimine-impregnated mesoporous silica: Effect of amine loading and surface alkyl chains on CO₂ adsorption, *Langmuir* 20 (2011) 12411–12416.
- [20] S. Deng, Y.P. Ting, Fungal biomass with grafted poly (acrylic acid) for enhancement of Cu(II) and Cd(II) biosorption, *Langmuir* 13 (2005) 5940–5948.
- [21] Z. Wang, X. Liu, M. Lv, J. Meng, Simple synthesis of magnetic mesoporous FeNi/carbon composites with a large capacity for the immobilization of biomolecules, *Carbon* 11 (2010) 3182–3189.
- [22] D. Zhao, Q. Huo, J. Feng, B.F. Chmelka, G.D. Stucky, Nonionic triblock and star diblock copolymer and oligomeric surfactant syntheses of highly ordered, hydrothermally stable, mesoporous silica structures, *J. Am. Chem. Soc.* 24 (1998) 6024–6036.
- [23] H.I. Lee, Y. Jung, S. Kim, J.A. Yoon, J.H. Kim, J.S. Hwang, M.H. Yun, J.-W. Yeon, C.S. Hong, J.M. Kim, Preparation and application of chelating polymer-mesoporous carbon composite for copper-ion adsorption, *Carbon* 4 (2009) 1043–1049.
- [24] M. Sevilla, P. Valle-Vigón, P. Tartaj, A.B. Fuertes, Magnetically separable bimodal mesoporous carbons with a large capacity for the immobilization of biomolecules, *Carbon* 10 (2009) 2519–2527.
- [25] Y. Liu, Z. Zeng, G. Zeng, L. Tang, Y. Pang, Z. Li, C. Liu, X. Lei, M. Wu, P. Ren, Immobilization of laccase on magnetic bimodal mesoporous carbon and the application in the removal of phenolic compounds, *Bioresour. Technol.* (2012) 21–26.
- [26] S.H. Huang, D.H. Chen, Rapid removal of heavy metal cations and anions from aqueous solutions by an amino-functionalized magnetic nano-adsorbent, *J. Hazard. Mater.* 1 (2009) 174–179.
- [27] X. Deng, L. Lü, H. Li, F. Luo, The adsorption properties of Pb(II) and Cd(II) on functionalized graphene prepared by electrolysis method, *J. Hazard. Mater.* 1 (2010) 923–930.
- [28] B. Manna, U.C. Ghosh, Adsorption of arsenic from aqueous solution on synthetic hydrous stannic oxide, *J. Hazard. Mater.* 1 (2007) 522–531.
- [29] Y. Pang, G. Zeng, L. Tang, Y. Zhang, Y. Liu, X. Lei, Z. Li, J. Zhang, G. Xie, PEI-grafted magnetic porous powder for highly effective adsorption of heavy metal ions, *Desalination* (2011) 278–284.
- [30] L. Xiong, C. Chen, Q. Chen, J. Ni, Adsorption of Pb(II) and Cd(II) from aqueous solutions using titanate nanotubes prepared via hydrothermal method, *J. Hazard. Mater.* 3 (2011) 741–748.
- [31] W. Li, S. Zhang, X.Q. Shan, Surface modification of goethite by phosphate for enhancement of Cu and Cd adsorption, *Colloids Surf., A* 1 (2007) 13–19.
- [32] B. Gao, Y. Gao, Y. Li, Preparation and chelation adsorption property of composite chelating material poly (amidoxime)/SiO₂ towards heavy metal ions, *Chem. Eng. J.* 3 (2010) 542–549.
- [33] T. Anirudhan, M. Ramachandran, Adsorptive removal of tannin from aqueous solutions by cationic surfactant-modified bentonite clay, *J. Colloid Interface Sci.* 1 (2006) 116–124.
- [34] G.D. Yang, L. Tang, X.X. Lei, G.M. Zeng, Y. Cai, X. Wei, Y.Y. Zhou, S.S. Li, Y. Fang, Y. Zhang, Cd(II) removal from aqueous solution by adsorption on α -ketoglutaric acid-modified magnetic chitosan, *Appl. Surf. Sci.* 292 (2014) 710–716.
- [35] M.B. McBride, A critique of diffuse double layer models applied to colloid and surface chemistry, *Clays Clay Miner.* 4 (1997) 598–608.
- [36] Y.H. Li, S. Wang, Z. Luan, J. Ding, C. Xu, D. Wu, Adsorption of cadmium(II) from aqueous solution by surface oxidized carbon nanotubes, *Carbon* 5 (2003) 1057–1062.
- [37] T.K. Naiya, A.K. Bhattacharya, S.K. Das, Adsorption of Cd(II) and Pb(II) from aqueous solutions on activated alumina, *J. Colloid Interface Sci.* 1 (2009) 14–26.
- [38] K. Kadirvelu, C. Namasivayam, Activated carbon from coconut coirpith as metal adsorbent: adsorption of Cd(II) from aqueous solution, *Adv. Environ. Res.* 2 (2003) 471–478.
- [39] A. Saeed, M. Iqbal, W.H. Höll, Kinetics, equilibrium and mechanism of Cd²⁺ removal from aqueous solution by mungbean husk, *J. Hazard. Mater.* 2 (2009) 1467–1475.
- [40] K.F. Lam, K.L. Yeung, G. McKay, Efficient approach for Cd²⁺ and Ni²⁺ removal and recovery using mesoporous adsorbent with tunable selectivity, *Environ. Sci. Technol.* 9 (2007) 3329–3334.